Modeling and Stability of PERT

Yueping Zhang
yueping@cs.tamu.edu

I. System Model

Our modeling of PERT is composed of three parts: window adjustment, RED emulation, and queuing behavior. We start with the window dynamics. Similar to [7], we consider a single-link scenario and assume the forward propagation delay from the source to the router is negligible and thus the round-trip time $R(t)$ measured by the end-user at time t is composed of backward propagation delay T_p and queuing delay $T_q(t-R(t))$, i.e.,

$$R(t) = T_p + T_q\big(t - R(t)\big). \tag{1}$$

Denoting by C the link's capacity and by $q(t)$ the queue size at time t, queuing delay $T_q(t)$ can be approximated by $q(t-R(t))/C$. Note that delay $R(t)$ in the last expression is because the queuing delay perceived by the user at time t is actually experienced by the router $R(t)$ time units earlier. Then, window dynamics of a PERT end-flow is written as:

$$\dot{W}(t) = \frac{1}{R(t)} - \frac{W(t)W\big(t-R(t)\big)}{2R\big(t-R(t)\big)}p(t), \tag{2}$$

where, at time t, $W(t)$ is the congestion window size, $R(t)$ is the RTT, and $p(t)$ is the packet dropping probability. Note that loss rate $p(t)$ in the last equation is an instantaneous value as appose to its delayed counterpart $p(t-R(t))$ in the TCP/RED model obtained in [7]. This is because a PERT user makes its dropping decision at the end-host instead of the router.

To formulate PERT's emulation of the RED mechanism, assume that the propagation delay T_p is known to the end-flow (this can be approximated by the base RTT). Then, upon each packet arrival, the user can estimate the queuing delay by $T_q(t) = R(t) - T_p$ and generate the packet drop probability $p(t)$ as following:

$$p(t) = \frac{T_q(t) - T_{min}}{T_{max} - T_{min}} p_{max}, \tag{3}$$

where T_{min} and T_{max} are the maximum and minimum thresholds of queuing delays and p_{max} is a constant.

Another component of RED emulation is the estimation of round-trip time $R(t)$, which is updated per-packet using a low-pass filter (LPF) with weight α, i.e.,

$$R(t) = \alpha R(t-1) + (1-\alpha)\hat{R}(t), \tag{4}$$

where $\hat{R}(t)$ is the instantaneous RTT measured at time t and weight $\alpha = 0.99$. Following the technique used in [7], this LPF can be approximated by the following differential equation:

$$\dot{R}(t) = \frac{\ln \alpha}{\delta}(R(t) - \hat{R}(t)), \tag{5}$$

where δ is the sampling interval.

We next model the queuing dynamics, which can be described by the following differential equation of queue size:

$$\dot{q}(t) = \frac{W(t)}{R(t)}N(t) - C,$$

where $N(t)$ is the number of flows accessing the router at time t and term $W(t)N(t)/R(t)$ can be interpreted as the combined incoming rate $y(t)$. Since $T_q(t) = q(t-R(t))/C$, we re-write the last equation in terms of queuing delay $T_q(t)$:

$$\dot{T}_q(t) = \frac{W(t-R(t))N(t-R(t))}{R(t-R(t))C} - 1. \tag{6}$$

Then, equations (1)-(6) comprise the complete system model of PERT. It is easy to see that this model is very similar to the TCP/RED model derived in [7]. Note that, there are also some differences between the system models of PERT and TCP/RED. The first one is that, in PERT, loss rate p in (2) is not delayed by $R(t)$ and variables for computing queuing delay T_q in (6) are retarded by one RTT. As we have mentioned earlier, this difference is because PERT monitors queuing dynamics at the end-user, while RED does this inside the router. The second difference is that PERT uses queuing delay $T_q(t)$ to determine loss probability, while RED uses queue length $q(t)$. We next study stability of PERT (1)-(6).

II. Stability Analysis

A. Stability Result

Similar to [7], we assume that the number of flows N and RTT R are constant in the steady state. Then, the system becomes:

$$\begin{aligned} f(W, W_R, T_q, p) &= \frac{1}{R} - \frac{W(t)W_R(t)}{2R}p(t), \\ g(W, T_q) &= \frac{N}{RC}W(t) - 1, \end{aligned} \tag{7}$$

where $W_R(t) = W(t-R)$. In the steady state, we have $W(t) = W_R(t) = W^*$. Applying this result and equating the left-hand sides of (7) to zero, we can derive the equilibrium point (W^*, p^*, T_q^*) as follows:

$$W^* = \frac{RC}{N} \text{ and } p^* = \frac{2N^2}{R^2C^2}. \tag{8}$$

The following theorem states a sufficient condition for PERT (7) to be locally stable in its stationary point.

Theorem 1: Let L_{PERT} and K be defined as follows:

$$L_{PERT} = \frac{p_{max}}{T_{max} - T_{min}}, \quad K = \frac{\ln \alpha}{\delta}, \tag{9}$$

and assume bounds R^+ and N^- satisfy the following condition:

$$\frac{L_{PERT}R^{+3}C^2}{(2N^-)^2} \le \sqrt{\frac{w_g^2}{K^2} + 1}, \tag{10}$$

where:

$$w_g = 0.1 \min\Big(\frac{2N^-}{R^{+2}C}, \frac{1}{R^+}\Big). \quad (11)$$

Then, PERT modeled by (7) is locally stable for all $N \geq N^-$ and $R^* \leq R^+$.

Proof: To determine local stability of the system, we first linearize it in the equilibrium:

$$\delta\dot{W}(t) = \frac{\partial f}{\partial W}\delta W(t) + \frac{\partial f}{\partial W_R}\delta W_R(t) + \frac{\partial f}{\partial p}\delta p(t) + \frac{\partial f}{\partial T_q}\delta T_q(t),$$

and

$$\delta\dot{p}(t) = \frac{\partial g}{\partial W}\delta W(t) + \frac{\partial g}{\partial T_q}\delta T_q(t),$$

where $\delta W(t) = W(t) - W^*$, $\delta W_R(t) = W_R(t) - W^*$, $\delta p(t) = p(t) - p^*$, $\delta T_q(t) = T_q(t) - T_q^*$, and the partial derivatives are given below:

$$\frac{\partial f}{\partial W} = \frac{\partial f}{\partial W_R} = -\frac{W^* p^*}{2R^*} = -\frac{N}{R^{*2}C}, \quad (12)$$

$$\frac{\partial f}{\partial p} = -\frac{W^{*2}}{2R^*} = -\frac{R^* C^2}{2N^2}, \quad (13)$$

$$\frac{\partial f}{\partial T_q} = -\frac{1}{R^{*2}} + \frac{W^{*2} p^*}{2R^{*2}} = 0, \quad (14)$$

$$\frac{\partial g}{\partial W} = \frac{N}{R^* C}, \quad (15)$$

and

$$\frac{\partial g}{\partial T_q} = -\frac{NW^*}{R^{*2}C} = -\frac{1}{R^*}. \quad (16)$$

Using approximation $W(t) = W_R(t)$ as in [7], the linearized PERT model becomes:

$$\delta\dot{W}(t) = -\frac{2N}{R^{*2}C}\delta W(t) - \frac{R^* C^2}{2N^2}\delta p(t), \quad (17)$$

$$\delta\dot{T}_q(t) = \frac{N}{R^* C}\delta W(t) - \frac{1}{R^*}\delta T_q(t). \quad (18)$$

Taking Laplace transforms of both sides of the last two equations, we obtain the following transfer functions:

$$P_W(s) = -\frac{\frac{R^* C^2}{2N^2}}{s + \frac{2N}{R^{*2}C}}, \quad (19)$$

and

$$P_T = \frac{\frac{N}{R^* C}}{s + \frac{1}{R^*}}. \quad (20)$$

Further notice that, according to [7], the transfer function of RED emulation (3)-(4) in PERT is:

$$C(s) = \frac{L_{PERT}}{s/K + 1}. \quad (21)$$

Combining (19)-(21) with the delay term e^{-sR^*} in the return path, we have the following closed-loop transfer-function model of PERT:

$$L(s) = P_W(s)P_T(s)C(s)e^{-sR^*} = -\frac{\frac{C}{2N}e^{-sR^*}L_{PERT}}{(s + \frac{2N}{R^{*2}C})(s + \frac{1}{R^*})(\frac{s}{K} + 1)}. \quad (22)$$

The rest of the proof directly follows from that of [4, Proposition 1]. ■

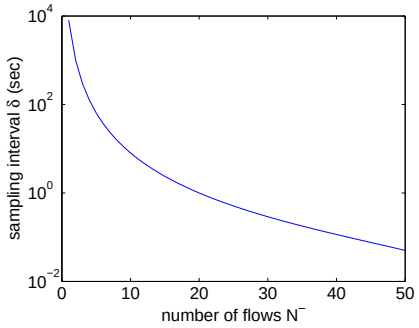

Fig. 2. Sampling interval δ as a function of the minimum number of flows N^-.

Note that, in addition to conditions given in Theorem 1, the equilibrium condition $p^* \leq p_{max}$ is also necessary for the system to be stable. To examine validity of this condition, we infer from (8) that $p^* = 2/(W^*)^2$. Thus, condition $p^* \leq p_{max}$ holds if and only if $p_{max} \geq 2/(W^*)^2$. For a stationary window size $W^* = 10$ packets, we have $p_{max} = 2\%$, which is reasonable in practice.

We next investigate whether there exists a closed-form solution of condition (10)-(11). Recalling $K = \ln\alpha/\delta$, we convert (10) into the following condition on δ:

$$\delta \geq -\frac{\ln\alpha}{4(N^-)^2 w_g}\sqrt{L_{PERT}^2 R^{+6} C^4 - 16(N^-)^4}. \quad (23)$$

This equation can be used as the guideline for choosing sampling interval δ given C, R^+, and N^-.

Moreover, we observe that given R^+ and C, δ scales inversely proportional to N. To better see this, consider the following simulation, where RTT $R = 200$ ms, packet size $s = 1250$ bytes, $p_{max} = 0.1$, $T_{max} = 100$ ms, $T_{min} = 50$ ms, and $\alpha = 0.99$. We set $C = 10$ mb/s (which corresponds to 1000 pkts/s) and range N^- from 1 to 50 to see the minimum requirement of δ. As seen from Figure 2, the minimum δ monotonically decreases and reaches 0.1 seconds as N^- goes to 40. We note that N^- is the lower bound of N. Thus, once a stable δ is picked given certain N^-, R^+, and C, stability of the system is not affected by N or R as long as $N \geq N^-$ and $R \leq R^+$.

B. Matlab Simulations

We next examine this stability condition using Matlab simulations. Bringing in notations $R(t) = R$, $x_1(t) = W(t)$, $x_2(t) = \hat{R}_q(t)$, and $x_3(t) = R_q(t)$, the fluid model of PERT (1)-(6) can be transformed into the following delay differential equations (DDEs):

$$\begin{aligned} \dot{x}_1(t) &= \frac{1}{R} - \frac{L_{PERT} x_1(t) x_1(t-R)(x_3(t-R) - T_{min})}{2R}, \\ \dot{x}_2(t) &= \frac{N}{RC}x_1(t) - 1, \\ \dot{x}_3(t) &= Kx_3(t) - Kx_2(t), \end{aligned} \quad (24)$$

where K and L_{PERT} are defined in (9).

Set link capacity $C = 100$ pkt/s (or 1 mb/s with packet size 1250 bytes), $\delta = 0.1$ ms, $N = N^- = 5$, $p_{max} = 0.1$,

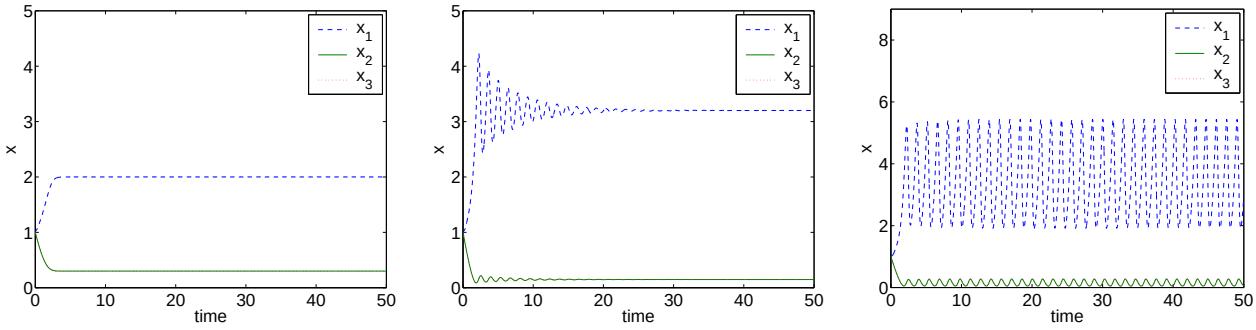

(a) $R = 100$ ms (b) $R = 160$ ms (c) $R = 171$ ms

Fig. 1. The fluid model of PERT (1)-(6) under different delay R.

$T_{max} = 100$ ms, $T_{min} = 50$ ms, and $\alpha = 0.99$. We keep $R = R^+$ and test stability of (24) under different values of delay R. For all simulations, we set the initial point to be $(1, 1, 1)$ and the unit of $x_1(t)$ is packets and that of $x_2(t)$ and $x_3(t)$ are both seconds. Start with $R = 100$ ms, which satisfies the stability condition in Theorem 1. As illustrated in Figure 1(a), the system is stable with monotonic trajectories. We then increase R to 160 ms, which is closer to the stability boundary, but still satisfies the stability condition. As shown in Figure 1(b), the system is stable and converges to its equilibrium (8) after decaying oscillations. Finally, we increase R to 171 ms, which is exactly on the stability boundary. As seen from Figure 1(c), the system is unstable and exhibits persistent oscillations, whose amplitude increases with the value of R. Note that the stability boundary derived from Theorem 1 is not exact. Even when R is within the stability region but close enough to the boundary, the system becomes unstable.

This discrepancy is due to the approximations $W(t) = W(t - R(t))$ in the proof. To justify this reasoning, we re-write (24) using $W(t) = W(t - R(t))$ and repeat the above simulations. The simulation results demonstrate that stability of the system is guaranteed under condition (10) and becomes unstable when R is increased to 175 ms (which exceeds the stability boundary 171 ms). Lack of necessity of the stability condition is also pointed out in the context of TCP/RED in [4]. However, Theorem 1 still serves as a general guideline for choosing PERT parameters.

C. Discussion

We remark on two differences between Theorem 1 and [7, Proposition 1]. The first one is that in the left-hand side of (10), we have C^2 instead of C^3 as in [7, (8)]. This is because PERT uses queuing delay $T_q(t)$ to determine loss probability, while RED uses queue size $q(t)$. Applying $L_{PERT} = L_{RED}C$ in (10), it is evident that the resulting stability condition is identical to that of RED.

The second difference is that sampling interval δ in RED is approximately fixed to $1/C$, while in PERT δ of user i is the inter-packet arrival time $1/x_i(t)$, which is approximately N/C. As a consequence, for fixed C, the more flows are accessing the bottleneck link, the slower the sampling action of each flow. Reflected in the stability condition, this also results in less constraint on C, R^+, and N^- than in RED. Thus, both differences actually increase the stability region of PERT. On the other hand, when the frequency of sampling action becomes extremely low, RTT estimation at the end user may not accurately capture the queuing dynamics inside the router. However, we argue that this problem does not occur in practice, since the ISP will increase link capacity as the number of accessing flows becomes large to decrease packet loss rate and prevent end-flows from starving. Thus, there are always sufficient packets within one RTT of each flow such that the end-user has enough samples for RTT estimation.

In addition, it is common to assume that link capacity C scales linearly with the number of flows N [2], i.e., $C/N = \sigma$, where σ is constant. Then, assuming $W^* \geq 2$, $N = N^-$, and $R = R^+$, condition (10)-(11) translates into:

$$L_{PERT}\sigma^2 R^+ \leq 4\sqrt{\frac{0.04}{\sigma^2 K^2 R^{+4}} + 1}, \tag{25}$$

which is independent of C and N^- and is only a function of R^+. This property does not hold for RED due to term C^3 instead of C^2 in (10). As a consequence, sampling interval δ of RED depends on (and thus unscalable to) C even if C/N is kept constant.

We should also note that, similar to RED, sampling interval δ in PERT also depends on the link capacity C and packet size s. Specifically, δ becomes small when C increases or s decreases and becomes large otherwise. As pointed out in [7], this adaptive nature of δ is harmful since small δ results in close tracking of the instantaneous queue length and thus leads to large oscillations. On the other hand, large δ results in increased rise time and extended initial overshoot of the queue length. Thus, it is suggested that δ be set to a fixed value that is independent of C, s, and N. As mentioned above, this requirement can be easily satisfied when ratio C/N is kept constant. A detailed discussion of the impact of δ on system performance is available in [7, Section 3.4].

III. Emulating PI

It has been identified that RED has several drawbacks, such as lack of significant performance improvement for pure web traffic [1] and mixtures of FTP, UDP and HTTP traffic [6], difficulties in tuning RED parameters [1], [3], [7], and tradeoff between stability and responsiveness of the system [7]. As pointed out in [5], the major cause of the last drawback

in the above list is the averaging mechanism of the LPF. Thus, the authors suggest using the instantaneous queue length and applying a PI controller to it. Simulation results in [5] demonstrate that PI offers better performance than RED in terms of stability and stationary queue size. Motivated by this fact, we next seek to emulate PI inside PERT.

The transfer function of PI is:

$$C_{PI}(s) = \frac{\Delta P(s)}{\Delta T_q(s)} = K\frac{1+s/m}{s}, \tag{26}$$

where $\Delta P(s)$ and $\Delta T_q(s)$ are respectively the Laplace transforms of $\delta p(t) = p(t) - p^*$ and $\delta T_q(t) = T_q(t) - T_q^*$ and K and m are constants to be determined next. Assuming $p^* = 0$, we re-write PI (26) in the time-domain as follows:

$$\delta p(t) = p(t) = K\Big(\delta T_q(t) + \frac{1}{m}\int \delta T_q(t)dt\Big). \tag{27}$$

To implement the continuous PI (27) in PERT, we discretize it using bilinear transform $s = 2(z-1)/\delta(z+1)$, where δ is the sampling interval, and convert the s-domain transfer function given in (26) into its following counterpart in the z-domain:

$$C_{PI}(z) = \frac{\Delta P(z)}{\Delta T_q(z)} = \frac{\gamma z - \beta}{z-1}, \tag{28}$$

where $\gamma = K/m + K\delta/2$ and $\beta = K/m - K\delta/2$. Then, the time-domain version of the PI controller becomes:

$$p(t) = \gamma(T_q(t) - T_q^*) - \beta(T_q(t-1) - T_q^*) + p(t-1), \tag{29}$$

Thus, in the new version of PERT, the only change is to replace RED emulation (3)-(4) with the PI controller (29).

Stability condition of PERT/PI defined by (7) and (29) is given below.

Theorem 2: Assume:

$$W^* \gg 2, \tag{30}$$

where W^* is the stationary window size. Then, PERT/PI defined by (7) and (29) with

$$m = \frac{2N^-}{R^{+2}C} \quad \text{and} \quad K = m\left|\frac{jR^*m+1}{\frac{R^{+3}C^2}{(2N^-)^2}}\right|, \tag{31}$$

is locally stable for all flow numbers $N \geq N^-$ and all stationary RTT $R^* \leq R^+$. Furthermore, the phase margin PM satisfies:

$$PM \approx 90^\circ - \frac{180}{\pi}m^2. \tag{32}$$

Proof: Following Theorem 1 and [5, Proposition 2], it is easy to prove that PERT/PI modeled by (7) and (27) with K and m defined in (31) is stable. Since stability is preserved under bilinear transform, stability condition of PERT (7) with discrete PI (29) is the same as that of (7) and (27). ■

Similar to Theorem 1, since PERT uses queuing delay to determine loss probability, in parameter K (31), we have term C^2 instead of C^3 as in the original stability condition of TCP/PI [5, Proposition 2]. In addition, it is clear that this controller is easy to implement and does not require a complicated tuning process of parameters such as T_{min}, T_{max}, p_{max} and α as in RED.

IV. PERT-V2

In this section, we present modeling and stability analysis of a variation of PERT, which we call PERT-V2, such that the resulting protocol can fairly compete with TCP SACK. The idea is to dynamically adjust the additive increase parameter α based on PERT's early dropping probability p' and the link's packet loss probability p. Now, the combined packet loss rate p_{PERT} experienced by the end-user becomes $p_{PERT} = 1 - (1-p')(1-p) = p + p' - pp'$. To roughly match the throughput equations of PERT and non-PERT TCP flows, we want to equate term $\beta p_{PERT}/\alpha_{PERT}$ and $\beta p/\alpha$. Since $\alpha = 1$ for the regular TCP, we have $\alpha_{PERT} = p_{PERT}/p = 1 + p'/p - p'$. Assuming $p' \ll 1$, we simplify the last equation as $\alpha_{PERT} = 1 + p'/p$.

We next analyze stability of the new method. Assuming loss rate $p = p^*$ at links is constant, we can rewrite steady-state equations of the system as following:

$$\begin{aligned} \frac{(1+p'/p^*)}{R} - \frac{W^2(p' + p^* - p'p^*)}{2R} &= 0, \\ \frac{NW}{RC} - 1 &= 0. \end{aligned} \tag{33}$$

Then, we have the following stationary values:

$$W^* = \frac{RC}{N} \text{ and } p'^* = \frac{R^2C^2p^{*2} - 2N^2p^*}{2N^2 - R^2C^2p^* + R^2C^2p^{*2}}. \tag{34}$$

Local stability of PERT-V2 is given in the following theorem.

Theorem 3: Let L_{PERT} and K be defined as follows:

$$L_{PERT} = \frac{p_{max}}{T_{max} - T_{min}}, \quad K = \frac{\ln\alpha}{\delta}, \tag{35}$$

and assume bounds R^+ and N^- satisfy the following condition:

$$\frac{L_{PERT}R^+C(1-p^*)\big(2(N^-)^2 - (R^+)^2C^2p^* + (R^+)^2C^2p^{*2}\big)}{4(N^-)^2Cp^{*2}} \leq \sqrt{\frac{w_g^2}{K^2}+1}, \tag{36}$$

where:

$$w_g = 0.1\min\Big(\frac{2N^-Cp^{*2}}{2(N^-)^2 - (R^+)^2C^2p^* + (R^+)^2C^2p^{*2}}, \frac{1}{R^+}\Big),$$

and link loss rate p^* is assumed to be constant. Then, PERT modeled by (7) is locally stable for all $N \geq N^-$ and $R^* \leq R^+$.

Proof: Linearizing the system in its equilibrium, we have:

$$\delta\dot{W}(t) = \frac{\partial f}{\partial W}\delta W(t) + \frac{\partial f}{\partial W_R}\delta W_R(t) + \frac{\partial f}{\partial p'}\delta p'(t) + \frac{\partial f}{\partial T_q}\delta T_q(t),$$

and

$$\delta\dot{p}'(t) = \frac{\partial g}{\partial W}\delta W(t) + \frac{\partial g}{\partial T_q}\delta T_q(t),$$

where $\delta W(t) = W(t) - W^*$, $\delta W_R(t) = W_R(t) - W^*$, $\delta p'(t) = p'(t) - p'^*$, $\delta T_q(t) = T_q(t) - T_q^*$, and the partial

derivatives are given below:

$$\frac{\partial f}{\partial W} = \frac{\partial f}{\partial W_R} = -\frac{W^*(p'^* + p^* - p'^* p^*)}{2R^*} = -\frac{NCp^{*2}}{2N^2 - R^2C^2p^* + R^2C^2p^{*2}}, \quad (37)$$

$$\frac{\partial f}{\partial p'} = -\frac{W^*(1-p^*)}{2R^*} = -\frac{R^*C^2(1-p^*)}{2N^2}, \quad (38)$$

$$\frac{\partial f}{\partial T_q} = -\frac{p'^* + p^*}{p^* R^{*2}} + \frac{W^{*2}(p'^* + p^* - p'^* p^*)}{2R^{*2}} = 0, \quad (39)$$

$$\frac{\partial g}{\partial W} = \frac{N}{R^* C}, \quad (40)$$

and

$$\frac{\partial g}{\partial T_q} = -\frac{NW^*}{R^{*2}C} = -\frac{1}{R^*}. \quad (41)$$

Using approximation $W(t) = W_R(t)$ as in [7], the linearized PERT model becomes:

$$\delta\dot{W}(t) = -\frac{2NCp^{*2}}{2N^2 - R^2C^2p^* + R^2C^2p^{*2}}\delta W(t) - \frac{R^*C^2(1-p^*)}{2N^2}\delta p'(t), \quad (42)$$

$$\delta\dot{T}_q(t) = \frac{N}{R^*C}\delta W(t) - \frac{1}{R^*}\delta T_q(t). \quad (43)$$

Taking Laplace transforms of both sides of the last two equations, we obtain the following transfer functions:

$$P_W(s) = -\frac{\frac{R^*C^2(1-p^*)}{2N^2}}{s + \frac{2NCp^{*2}}{2N^2 - R^2C^2p^* + R^2C^2p^{*2}}}, \quad (44)$$

and

$$P_T(s) = \frac{\frac{N}{R^*C}}{s + \frac{1}{R^*}}. \quad (45)$$

Further notice that, according to [7], the transfer function of RED emulation (3)-(4) in PERT is:

$$C(s) = \frac{L_{PERT}}{s/K + 1}. \quad (46)$$

Combining the above equations with the delay term e^{-sR^*} in the return path, we have the following closed-loop transfer-function model of PERT:

$$L(s) = P_W(s)P_T(s)C(s)e^{-sR^*} \quad (47)$$
$$= -\frac{\frac{C(1-p^*)}{2N}e^{-sR^*}L_{PERT}}{(s + \frac{2NCp^{*2}}{2N^2 - R^2C^2p^* + R^2C^2p^{*2}})(s + \frac{1}{R^*})(\frac{s}{K} + 1)}.$$

The rest of the proof directly follows from that of [4, Proposition 1]. ■

V. PERT-V3

A. Analysis

In this section, we present and analyze a new version of PERT, which we call PERT-V3. In this new protocol, upon the onset of congestion the end-user reducing the congestion window by a factor of $\beta = T_q(t)/(T_q(t) + T_{max})$ instead of $\beta = 1/2$. In other words, the congestion window $W(t)$ becomes $(1-\beta)W(t)$ upon detection of a packet loss event. Thus, assuming the RTT $R(t) = R$ is constant, we can write the system equations as following:

$$f(t) = \dot{W}(t) = \frac{1}{R} - \frac{T_{max}W(t)W_R(t)}{(T_q(t) + T_{max})R}p(t), \quad (48)$$

$$g(t) = \dot{q}(t) = \frac{N}{RC}W(t) - 1. \quad (49)$$

Combining this model with equation $p(t) = L_{PERT}(T_q(t) - T_{min})$, we have:

$$W^* = \frac{RC}{N}, \quad (50)$$

$$T_q^* = \frac{T_{max}(N^2 + R^{*2}C^2L_{PERT}T_{min})}{T_{max}R^{*2}C^2L_{PERT} - N^2}, \quad (51)$$

$$p^* = \frac{L_{PERT}N^2(T_{max} + T_{min})}{T_{max}R^{*2}C^2L_{PERT} - N^2}. \quad (52)$$

We next attempt to study local stability of the system in its equilibrium (W^*, p^*, T_q^*).

Theorem 4: Let:

$$L_{PERT} = \frac{p_{max}}{T_{max} - T_{min}}, \quad K = \frac{\ln\alpha}{\delta}. \quad (53)$$

Assume bounds R^+ and N^- satisfy the following condition:

$$\frac{(T_{max}R^{+2}C^2L_{PERT} - N^{-2})^2}{2C^2N^{-2}L_{PERT}T_{max}(T_{max} + T_{min})} \leq \sqrt{\frac{w_g^2}{K^2} + 1}, \quad (54)$$

where:

$$w_g = 0.1\min\Big(\frac{2N^-}{R^{+2}C}, \frac{1}{R^+}\Big). \quad (55)$$

Then, PERT-V3 modeled by (48)-(49) is locally stable for all $N \geq N^-$ and $R^* \leq R^+$.

Proof: We first obtain the following partial derivatives:

$$\frac{\partial f}{\partial W} = \frac{\partial f}{\partial W_R} = -\frac{2W^*T_{max}}{(T_q^* + T_{max})R^*}p^* = -\frac{2N}{R^{*2}C}, \quad (56)$$

$$\frac{\partial f}{\partial p} = -\frac{1}{R^*p^*}, \quad (57)$$

$$\frac{\partial f}{\partial T_q} = \frac{1}{(T_q^* + T_{max})R^*}, \quad (58)$$

$$\frac{\partial g}{\partial W} = \frac{N}{R^*C}, \quad (59)$$

$$\frac{\partial g}{\partial T_q} = -\frac{1}{R^*}. \quad (60)$$

Then, the linearized window dynamics of PERT-V3 is given by the following differential equation:

$$\delta\dot{W}(t) = -\frac{2N}{R^{*2}C}\delta W(t) - \frac{1}{R^*p^*}\delta p(t) + \frac{1}{(T_q^* + T_{max})R^*}\delta T_q(t). \quad (61)$$

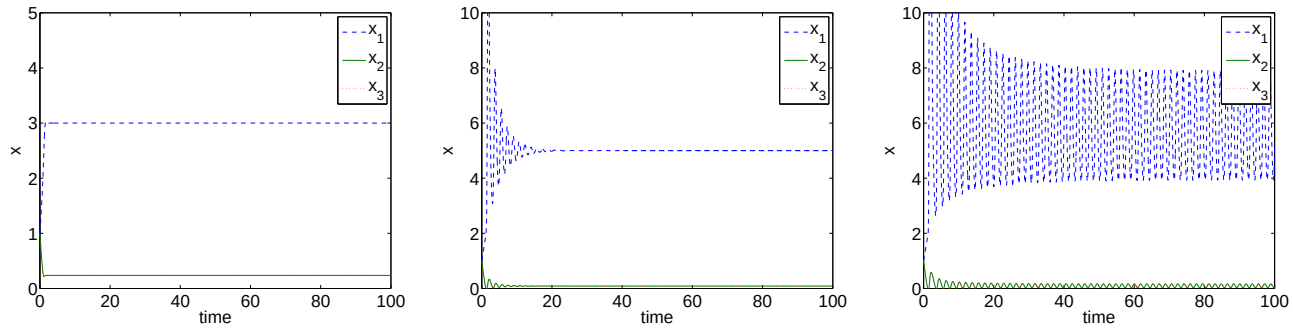

(a) $R = 150$ ms (b) $R = 250$ ms (c) $R = 270$ ms

Fig. 3. The fluid model of PERT-V3 under different delay R.

Further noticing that $T_q(t) = p(t)/L_{PERT} + T_{min}$, we have $T_q^* = p^*/L_{PERT} + T_{min}$ and $\delta p(t) = p(t) - p^* = \delta T_q(t)/L_{PERT}$. Then, we can rewrite (61) as:

$$\delta\dot{W}(t) = -\frac{2N}{R^{*2}C}\delta W(t) + \Gamma\delta p(t), \tag{62}$$

where

$$\Gamma = -\frac{(T_{max}R^{*2}C^2L_{PERT} - N^2)^2}{R^{*2}C^2N^2L_{PERT}T_{max}(T_{max} + T_{min})}. \tag{63}$$

Then, the s-domain transfer function of the last equation becomes:

$$P_W(s) = -\frac{\Gamma}{s + \frac{2N}{R^{*2}C}}. \tag{64}$$

The linearized equation of queuing dynamics is the same as before:

$$\delta\dot{q}(t) = \frac{N}{R^*C}\delta W(t) - \frac{1}{R^*}\delta T_q(t), \tag{65}$$

whose transfer function is easy to obtain:

$$P_T(s) = \frac{\frac{N}{R^*C}}{s + \frac{1}{R^*}}. \tag{66}$$

Following the previous techniques, we have the following closed-loop transfer function $L(s)$:

$$L(s) = \frac{\frac{N\Gamma}{R^*C}L_{PERT}e^{-sR^*}}{(s + \frac{2N}{R^{*2}C})(s + \frac{1}{R^*})(\frac{s}{K} + 1)}. \tag{67}$$

The rest of the proof directly follows from [4, Proposition 1]. ■

B. Simulation

We next examine this stability condition using Matlab simulations. Bringing in notations $R(t) = T_p + T_q(t)$, $x_1(t) = W(t)$, $x_2(t) = \hat{T}_q(t)$, and $x_3(t) = T_q(t)$, the fluid model of PERT-V3 can be transformed into the following delay differential equations:

$$\begin{aligned}
\dot{x}_1(t) &= \frac{1}{R(t)} - \frac{L_{PERT}x_1^2(t)T_{max}(x_3(t - R(t)) - T_{min})}{R(t)(T_q(t) + T_{max})}, \\
\dot{x}_2(t) &= \frac{N}{R(t)C}x_1(t) - 1, \\
\dot{x}_3(t) &= Kx_3(t) - Kx_2(t),
\end{aligned} \tag{68}$$

where K and L_{PERT} are defined in (9).

We use the same system setting as Figure 1, that is, link capacity $C = 100$ pkt/sec (or 1 mb/s with packet size 1250 bytes), $\delta = 0.1$ ms, $N = N^- = 5$, $p_{max} = 0.1$, $T_{max} = 100$ ms, $T_{min} = 50$ ms, and $\alpha = 0.99$. We keep $R = R^+$ and test stability of (68) under different values of delay R. For all simulations, we set the initial point to be $(1, 1, 1)$ and the unit of $x_1(t)$ is packets and that of $x_2(t)$ and $x_3(t)$ are both seconds. We start with $R = 150$ ms, which satisfies the stability condition in Theorem 4. As illustrated in Figure 3(a), PERT-V3 is stable with monotonic trajectories and converges the congestion window $W(t)$ exactly to the predicted value $W^* = 3$ packets. We then increase R to 250 ms, which is closer to the stability boundary, but still satisfies the stability condition. As shown in Figure 3(b), the system is stable and converges to its equilibrium $W^* = 5$ packets after decaying oscillations. Finally, we increase R to the stability boundary 270 ms. As seen from Figure 3(c), the system is marginally stable and exhibits persistent oscillations.

Comparing these results to Figure 1, we infer that under the same system configuration, PERT-V3 exhibits better stability properties and tolerates higher delay than the original PERT. In addition, we also observe from simulations that PERT-V3 has lower stationary queuing delay T_q^* and dropping rate p^* than PERT as well as preserving the steady-state congestion window W^*. All of these properties, combined its TCP friendliness, make PERT-V3 a better choice than PERT in practical settings.

REFERENCES

[1] M. Christiansen, K. Jeffay, D. Ott, and F. D. Smith, "Tuning RED for Web Traffic," in *Proc. ACM SIGCOMM*, Aug. 2000, pp. 139–150.

[2] A. Dhamdhere, H. Jiang, and C. Dovrolis, "Buffer Sizing for Congested Internet Links," in *Proc. IEEE INFOCOM*, Mar. 2005, pp. 1072–1083.

[3] S. Floyd, R. Gummadi, and S. Shenker, "Adaptive RED: An Algorithm for Increasing the Robustness of RED's Active Queue Management," ICIR, Tech. Rep., Aug. 2001.

[4] C. V. Hollot, V. Misra, D. Towsley, and W.-B. Gong, "A Control Theoretical Analysis of RED," in *Proc. IEEE INFOCOM*, Apr. 2001, pp. 1510–1519.

[5] C. V. Hollot, V. Misra, D. Towsley, and W.-B. Gong, "On Designing Improved Controllers for AQM Routers Supporting TCP Flows," in *Proc. IEEE INFOCOM*, Apr. 2001, pp. 1726–1734.

[6] M. May, J. Bolot, C. Diot, and B. Lyles, "Reasons Not to Deploy RED," in *Proc. IEEE IWQoS*, Jun. 1999, pp. 260–262.

[7] V. Misra, W.-B. Gong, and D. Towsley, "A Fluid-Based Analysis of a Network of AQM Routers Supporting TCP Flows with an Application to RED," in *Proc. ACM SIGCOMM*, Aug. 2000, pp. 151–160.